Nickel and Copper Electroplating of Patterned Carbon-Coated Carbon Nanotube Forests for Applications in Microelectricalmechanical Systems and Through-Silicon Vias

Dallin J. Barton

A senior thesis submitted to the faculty of
Brigham Young University
in partial fulfillment of the requirements for the degree of

Bachelor of Science

Richard Vanfleet, Advisor

Department of Physics and Astronomy

Brigham Young University

August 2015

Copyright © 2015 Dallin J. Barton

All Rights Reserved

ABSTRACT

Nickel and Copper Electroplating of Patterned Carbon-Coated Carbon Nanotube Forests for Applications in Microelectricalmechanical Systems and Through-Silicon Vias

Dallin J. Barton
Department of Physics and Astronomy, BYU
Bachelor of Science

This thesis presents processes and techniques of electroplating two different metals, nickel and copper, onto patterned ozone-treated carbon-coated carbon nanotube (CNT) forests. Through nickel-electroplating CNTs, we have created a new composite material. The Young's modulus of the nickel-electroplated CNT forest is $\sim$42 GPa with a tensile strength reaching 400 MPa and a density that is 85% of bulk nickel. Several different variables were tested to find the fullest and most uniform fill. The parameters used to find the most uniform fill include: a nickel chloride boric acid solution, temperature kept at 50 °C, pH between 3 and 4, current density of 8 mA/mm^3, pulsing with 3ms on 27ms off, agitation, electrical contact, anode of sulphur depolarized nickel rounds, ozone surface treatment, pre-soak time of 30 minutes, and run time of nine hours. The variables that yield the most uniform copper-electroplating results are similar to the variables that yield the most uniform nickel-electroplating results. A base copper solution without extra additives and with an electroplating process similar to nickel electroplating yields the most uniform electroplating so far.

Keywords: [Carbon Nanotube, Nickel Electroplating, Copper Electroplating, High-Aspect Ratio, Microelectricalmechanical Systems, Through-Silicon Vias]

ACKNOWLEDGMENTS

I would like to recognize the BYU Department of Physics and Astronomy and the BYU Mentored Environment Grant for funding at BYU, and the NSF REU Grant and EEC 1005191 Grant for funding at UA.

I would also like to thank like to thank Lawrence Barrett for training me on nearly everything (without exaggeration), Prof. David Allred for inspiring me to major in physics, Profs. Davis and Vanfleet for keeping me in physics, Jim Fraser, and the staff involved with BYU cleanroom, Paul Minson and Jeffrey Farrer for their microscopy training, Univertical for free nickel sulfamate solution and nickel S-rounds, Enthone for copper solutions, Rich Martens and the staff at University of Alabama (UA) Central Analytical Facility staff for their microscopy training, Prof. Susan Burkett and Dr. Ying Feng for training and mentoring at copper electroplating in UA. Prof. Robert M. Metzger and Prof. Shane Street of the Chemistry Department at UA for plasma and ozone generators, Jason Lund for Instron testing, and Berg Dodson and Alex Molina for helping in nickel electroplating and creating solutions. My family for their unwavering support, and God for giving me the strength to finish this out.

Contents

Table of Contents **iv**

List of Figures **vi**

1 Introduction **1**
1.1 Microelectricalmechanical Systems (MEMS) 2
1.2 Through-Silicon Vias (TSVs) 2

2 Nickel-Electroplating Methods **6**
2.1 Electroplating 6
2.2 Patterned Carbon Nanotube Forest (CNT) Growth and Carbon Infiltration 7
2.3 Ozone Treatment 8
2.4 Anode 8
2.5 Cathode 8
2.6 Nickel Solutions 10
2.7 Surface Treatment 11
2.8 Pulsing, Current Density, and Pre-Soak Time 14
2.9 Final Parameters 14
2.10 Material Properties 14
2.11 Instron Tensile Testing 17
2.12 Alternating Gradient Magnetometer (AGM) 17
2.13 Annealing 19

3 Copper-Electroplating **23**
3.1 Introduction 23
3.2 Preliminary Copper Solution 26
3.3 Ozone Treatment 26
3.4 More Copper Solutions 28

4 Future Work **35**
4.1 Ideas for Continuing Nickel 35
4.2 Ideas for Continuing Copper 36

4.3 Wrap-up 38

Appendix A Patterned Carbon Nanotube Forest Growth **39**

Bibliography **41**

Index **44**

List of Figures

1.1 Diagram of a MOSFET 4

1.2 Side-view diagram of TSVs. 4

2.1 CNT contact device. 6

2.2 CNT contact device. 9

2.3 Titanium basket with nickel cathodes 9

2.4 Nickel-Plated CNTs with nickel sulfamate bath. 12

2.5 Nickel-electroplated CNTs with a nickel chloride bath. 13

2.6 Ozone treated CNTs plated with a $NiCl_2$ bath with 350x and 3500x magnifications. 15

2.7 Magnetic hysteresis curve of nickel-plated CNTs 18

2.8 Top view of Polished Annealed Nickel-Electroplated CNTs 19

2.9 Side View of a Polished Annealed Nickel-Electroplated CNTs 20

2.10 Polished Nickel-Electroplated CNTs 20000x 20

2.11 Polished Nickel-Electroplated CNTs 80000x 21

2.12 A Sample of Polished Annealed Nickel-Electroplated CNTs with Orientation Imaging Microscopy 22

3.1 CNT contact device. 24

3.2 Copper-plated CNTs with SC MD and LO 70/30 solution 27

3.3 Plasma cleaned CNTs 28
3.4 Direct ozone treated CNTs 29
3.5 CNTs plated with a copper-bath with a base of MU 200-B and MU 200-C from Enthone. 31
3.6 Copper-plated CNTs with DVF MU 200 diluted 15:1 with deionized water and with 10g/l of boric acid added. 32
3.7 Copper-plated CNTs with DVF MU 200 diluted 121:1 with de-ionized water. . . . 33
3.8 Copper-plated CNTs with DVF MU 200 with no additives 34

List of Tables

2.1 Nickel-electroplating solutions and their results. 10

2.2 Current nickel-electroplating parameters for plating the forest with the most fill. . . 16

2.3 Material properties of nickel and silicon processes used for MEMS. 17

3.1 Final copper-plating parameters for plating the forest with the most fill. 25

Chapter 1

Introduction

This thesis presents methods of copper-electroplating and nickel-electroplating carbon infiltrated carbon nanotube (CNT) forests that have been patterned through photolithography. Applications and motivation will be introduced, followed by the work done in in both copper and nickel. Research in electroplating nickel-CNT composites and copper-CNT composites has been extensive and thorough. However, all of these papers have CNTs deposited with the metal onto a flat substrate. Our process includes plating metal on CNT structures still attached to the silicon substrate to which the CNTs were grown.

Some of our work of nickel-electroplating CNT forests is already published in a senior thesis authored by Lawrence Barrett [1] and an article in JMEMS [2]. Nickel-electroplated CNT forest material properties will be discussed including Young's modulus, tensile strength, and magnetic hysterisis. As less research concerning copper-electroplating CNT forests has been published, many of the basic copper electroplating parameters will be explored here.

1.1 Microelectricalmechanical Systems (MEMS)

The field of Microelectricalmechanical Systems (MEMS) is growing in several different consumer and industrial applications. They are present in smartphones, airbags, jetplanes, and many other devices that requires a micro-scaled system with both mechanical and electrical parts. While small electrical devices such as metal-oxide-semiconductor field-effect transistors (MOSFET)s are primarily electrical in nature, there is an increasing demand for micro-systems with a mechanical function such as sensors and actuators. Silicon, the commanding material in MEMS, is readily structured through photolithography, deep etching, and doping. However, analagous to trying to build and furnish a house only out of one material like granite, silicon has limitations in its usefulness. If a metal high-aspect-ratio MEMS fabrication process was available, the availability and usefulness of MEMS would increase.

Actuators provide an example of the utility of metal MEMS. Most MEMS actuators involve electrostatic forces. Electrostatics are useful and can be employed in several applications, but are inefficient at separation distances greater than two μm [3]. As the distance between electrostatic devices increases, the electrostatic field begins to breakdown exponentially. Magnetostatic forces are perferred over electrostatics once the separation distance exceeds two μm. With a nickel-composite material, it will now be possible to construct devices that can harness magnetism allowing for greater forces achieved.

1.2 Through-Silicon Vias (TSVs)

Transistors and integrated circuits have been some of the the most widespread and heavily distributed products since its invention in the twentieth century. Gordon Moore observed that the number of transistors will double every year from 1965 to 1975. He said, "The complexity for minimum component costs has increased at a rate of roughly a factor of two per year. Certainly

over the short term this rate can be expected to continue, if not to increase." [4] Semiconductor industries were able to meet this prediction and set it as a standard for technology development. Over the past fifty years, the amount of transistors on a silicon die continues to increase through miniaturization breakthroughs. [5]

Currently, the smallest common MOSFET is about 30nm in size [6] [7]. At this size there is a fundamentally difficult physical phenomenon to overcome, quantum tunneling. In a MOSFET, there is a source, a drain, and and a gate as shown in Figure 1.1. The source and drain are separated by the gate. The voltage applied to the gate determines whether the drain and source are tied together through a low impedance channel. As MOSFETs become smaller, distances between the drain and source decrease. MOSFETs are now so small that the electric field produced by gate voltage does not effectively separate the source and the drain. Electrons are tunneling through these channels. Power is also required to run through MOSFETs. As MOSFETs decrease in size, their density will increase. As a result, power density will also increase. Currently, the power density of a Pentium chip is around 10 W/cm^2, enough current density to power a hot plate. As current densities increase, power consumption and rising temperatures will cause serious limitations.

In order to continue to increase processing speed and reduce transistor sizes in our computers, a new piece of technology has emerged, three-dimensional (3D) integration. Die can be stacked on top of each other and connected. Normally, these separate die have a large distance between them and can experience latency, making it difficult to effectively connect multiple die into a small package. To address this problem, through-silicon vias (TSVs) are created to decrease the distance between silicon die. A TSV is created by placing copper columns inside of the silicon die allowing the components to be stacked. Current TSV technology have via dimensions with diameters ranging from 10-25 μm in diameter and a depth of 75-125 μm. As the copper posts are several times taller than they are wide, they are called a high-aspect ratio structure. Figure 1.2 illustrates a sample structure and functionality of TSVs.

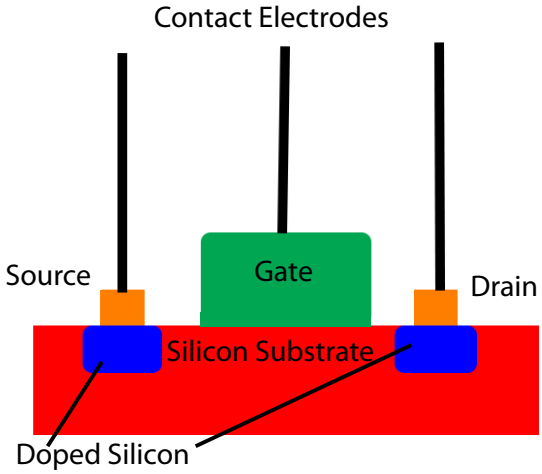


Figure 1.1 Diagram of a MOSFET. The limit of the MOSFET exists when the source and the drain are too close to each other. The electrons will tunnel through the insulation separating the source, gate, and drain, thus eliminating the ability for the MOSFET to act as a switch. This limit is reached as the distance between the source and the drain are in the tens of nm.

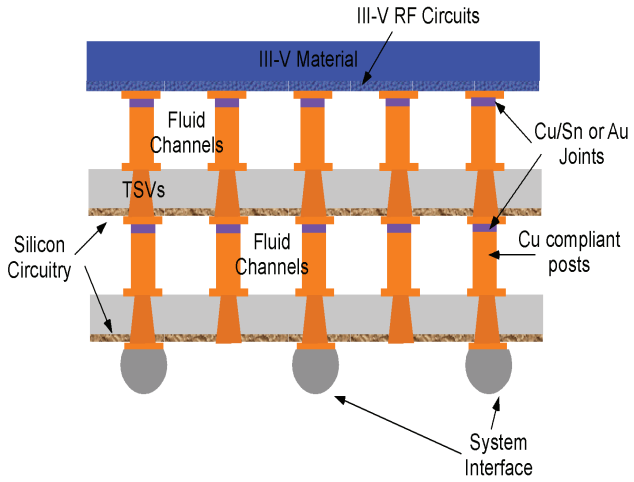


Figure 1.2 Side view diagram of TSVs. The copper posts are to provide cooling as the die are stacked. The copper through the silicon (hence the 'through silicon' part of 'through-silicon vias') provide an electrical connection in between the stacks of silicon. Figure used with permission by Prof. Susan Burkett. [8]

One of the leading problems in TSV technology is electromigration. As electricity is passed through the small structures, the electrons' momentum causes copper atoms to move. In a macroscopic scale this is hardly noticeable, but on a high-aspect-ratio micron scale, this leads to destruction of interconnects. Aluminum was used to be a common metal in electronic circuits, until Intel discovered a way to create circuits with copper. Copper is preferred over aluminum due to its conductivity, manufacturability, and resistance to electromigration. While copper is more resistant to electromigration, it is not completely immune and improvements in this area are desired.

Chapter 2

Nickel-Electroplating Methods

2.1 Electroplating

Electroplating is performed by putting a source of metal desired to be plated and a substrate in a solution bath containing the metal ions. A current is run through it. Metal from the source is taken off by the positive charge flowing through it. The negatively charged source, or anode then attract the positive ions floating in the solution. See Figure 2.1.

One of the major problems electroplating high-aspect-ratio structures is a phenomenon called

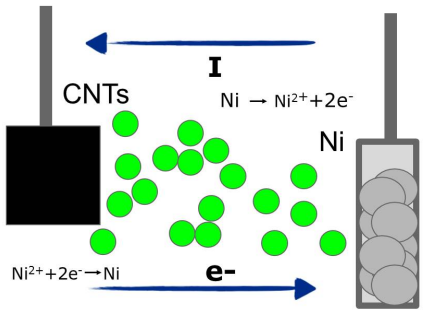


Figure 2.1 Diagram of how nickel electroplating works.

keyholing. On the top corners of the structure deposition rates are higher due to the increased surface area. The bottom of the deep structure, or pits, have a decreased exposed surface area and therefore lower electrodeposition. The top can close off the pit before it has a chance to fill in completely. As it is capped off, plating solution can no longer reach the bottom of the pit and there is a gap inside of the structure.

2.2 Patterned Carbon Nanotube Forest (CNT) Growth and Carbon Infiltration

Devices used in electroplated were created with CNT manufacturing. Using photolithography, iron can be laid down in a pattern on a silicon substrate coated with alumina. This patterned iron acts as a catalyst for ethylene to grow CNTs allowing for patterned CNTs. While strong, CNTs are easily disconnected from the substrate. CNTs are porous enough that the pattern does not hold once released from the substrate. Submerging the substrate into an electroplating bath often causes enough force to disconnect the CNTs. This problem is solved with carbon infiltration. Carbon infiltration is done by flowing ethylene at a high enough temperature to deposite nano-crystalline carbon. With differing times (or amounts) of carbon infiltration, CNT structures can have varying percentages of porosity with different strengths as studied by Hanna et al [9]. The CNTs used for electroplating have been infiltrated with carbon for two minutes at 900 °C. This provides enough carbon to keep the structure together while allowing enough porosity for nickel electroplating. The steps of growing CNTs are given in Appendix A.

2.3 Ozone Treatment

After being grown and infiltrated with carbon, CNTs are ozone treated through a process described by Jensen et al [10]. They are ozone treated to make the forests hydrophilic instead of hydrophobic. The hydrophilicity decreases the chance of air pockets. Hydrophobicity and hydrophilicity can be reversed [11]. While certain processes can affect the time of reversal, it was observed that CNT forests passively reverse from a hydrophilic state to a hydrophobic state after several weeks of sitting at standard temperature and pressure. To ensure the hydrophilicity of the CNTs, samples were electroplated within one week of ozone treatment.

2.4 Anode

Electrical contact was made by soldering a staple to an alligator clip. The entire clip with exception to the staple was then coated in nail polish with an ethyl acetate and butyl acetate base. Nail polish is electrically insulating and prevents electroplating wherever it is covering. The clip was directly clamped onto the CNTs. This is shown in Figure 2.2.

2.5 Cathode

The cathode was a titanium basket holding sulphur depolarized nickel rounds. Titanium does not electroplate or galvanically corrode as quickly compared to other metals making it a choice material for a cathode basket. The basket is shown in Figure 2.3. The sulphur impurity in the nickel cathode allowed for nickel to evenly dissolve from the solid into the solution with little regard to current density.



Figure 2.2 Electrically insulated contact device with a needle on the CNTs.



Figure 2.3 Titanium basket used in electroplating. The basket containing the nickel rounds are submerged in the solution and an electrical contact is made outside of the bath.

2.6 Nickel Solutions

Two different nickel-electroplating solutions were tested, a nickel sulfamate bath and a nickel chloride bath.

Solution	Chemical	Concentration (g/l)	Results
Nickel Sulfamate			Non-uniform Plating
	Nickel Sulfamate ($NiSO_4$)	14	
	Nickel Chloride ($NiCl_2$)	0.8	
	Boric Acid (H_3BO_3)	3.2	
	Sodium Sulfate (Na_2SO_4)	4.8	
	Saccharin ($NaC_{12}H_{25}SO_4$)	0.008	
Nickel Chloride			Uniform Plating
	Nickel Chloride Hexahydrate ($NiCl_2$*$6H_2O$)	125	
	Boric Acid (H_3BO_3)	12.5	

Table 2.1 Nickel-electroplating solutions and their results.

The most commonly used bath in nickel-electroplating is nickel sulfamate. Nickel sulfamate is the most common plating bath used in the electroplating industry because of its high throwing power and low internal stress. This means that nickel will plate quickly, and during plating, the electroplated metal will not pull on itself as strongly. This is also true for CNTs. Most commercial electroplating occurs at relatively low aspect-ratios, 5:1 or 10:1 at the most. The spacing in between CNTs are approximately 100 nm. With a structure height at around 100 μm, CNT structures can be seen as having aspect ratios of 100:1 Nickel sulfamate electroplates too fast capping the top of the forest preventing diffusion and a uniformly filled structure. The structure is brittle to the touch. This capping layer can be seen in Figures 2.4a and 2.4b. The figures are generated by taking a

nickel sulfamate sample, mechanically breaking it in half, and looking at a cross-sectional view in an scanning electron microscope (S-FEG SEM XL-30). Electroplating the tubes individually needs to have diffusion in mind.

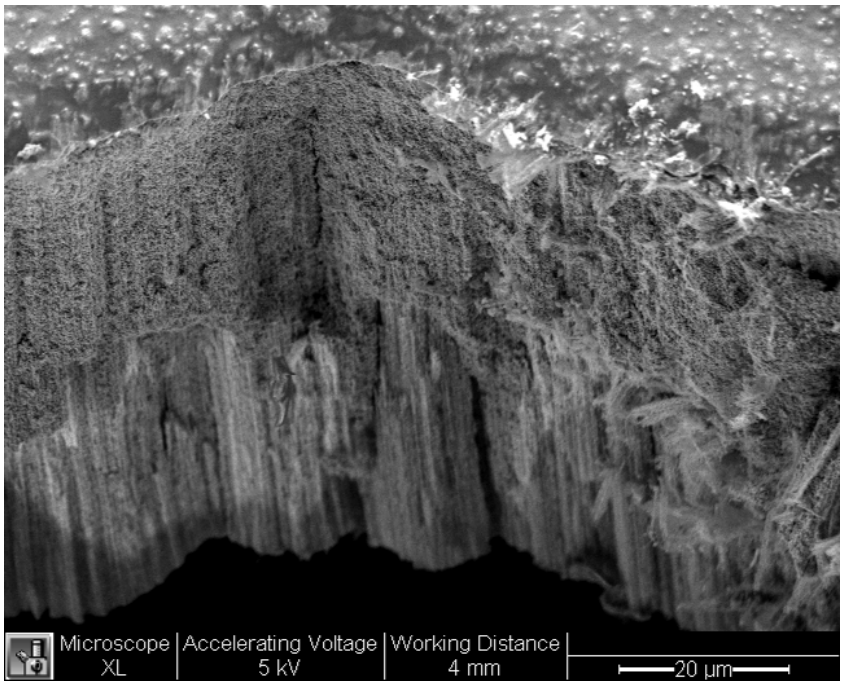
Because the CNTs were only partially filled, the forests were weak and brittle. They would break to the touch. As a result, we looked at different electroplating solutions that had slower electroplating rates and less internal stress. The pH of the bath can effect electroplating as it indicates the number of ions in a solution. Boric acid acts as a buffering reagent, minimizing pH change at current densities less than 1.0 A dm^{-2} [12] [13]. Nickel chloride results in slower nickel electroplating than the nickel sulfamate. Table 2.1 shows the two different baths used.

Nickel chloride baths resulted in more uniform nickel-electroplated CNTs. The results of these are shown in Figure 2.4b. Notice the triangular pockets and voids in the CNTs.

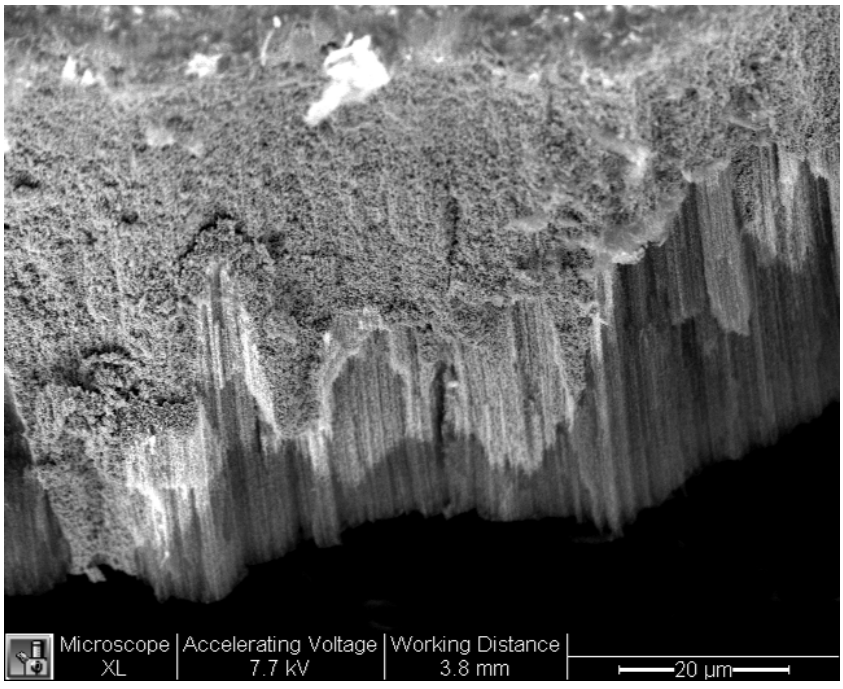
2.7 Surface Treatment

The nickel chloride solution had more uniform plating than the nickel sulfamate plating. However, there were large traingular voids. Figures 2.5a and 2.5b show examples of the voids. It is proposed that these voids are caused by air bubbles being trapped in the CNTs.

CNTs are hydrophobic, meaning that they repel water, after being grown. It is believed that the hydrophobicity of the CNTs cause air pockets near the bottom of the forest. These air bubbles prevent electroplating. CNTs are surfaced treated with ozone to make them hydrophilic, or attracted to water. If the CNTs are hydrophilic, the water based solution could be drawn into the forest easier, eliminating bubbles, and allowing for more uniform plating. CNTs have been surface treated with ozone through a process outlined by Jensen et al [10]. CNTs were placed in a 1 in. fused silica tube. The tube was connected to an Atlas 30 Ozone Generator (Absolute Ozone, Edmonton, Alberta). The oxygen rate was approximately one square cubic foot per hour (SCFH)

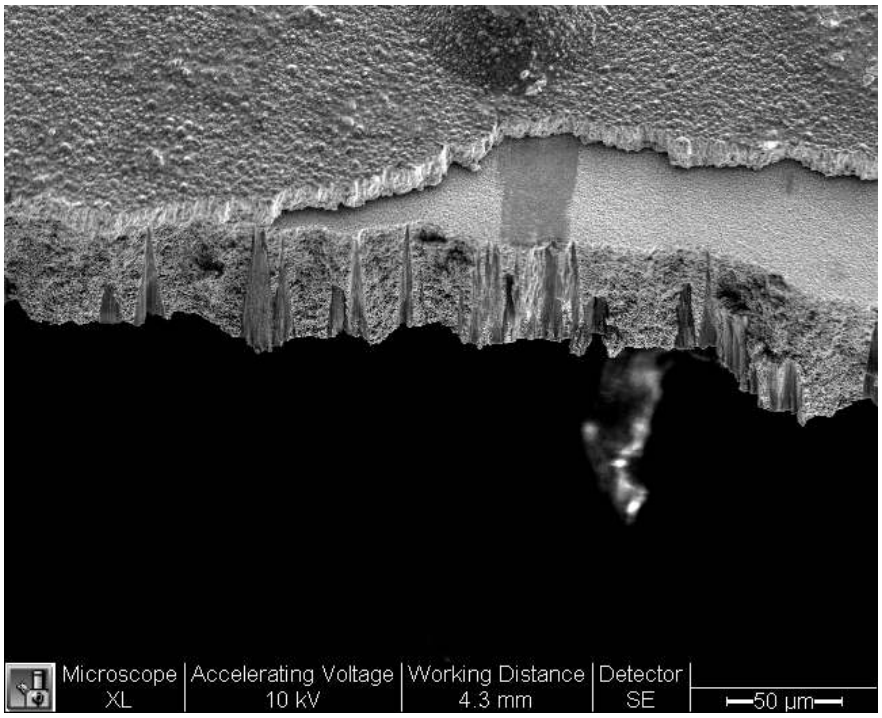


(a) The sample was cleaved in order to look at the side view cross-section. The solid part on top is the capping layer. Underneath, half-way down the forest are nickel particles, and the bottom is very sparsely plated with tubes showing through.

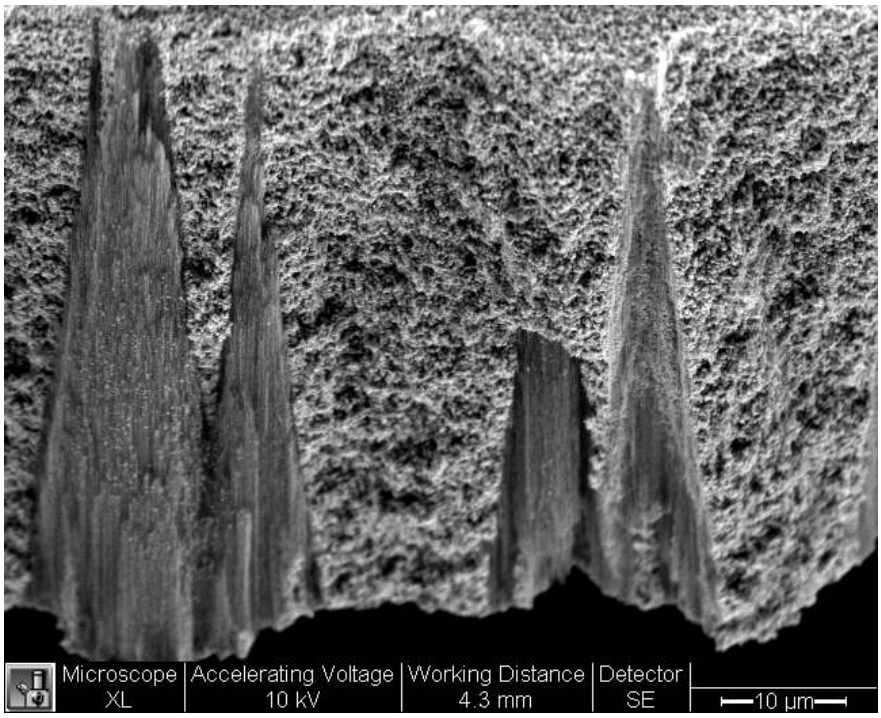


(b) A different view of the same sample. Notice the similar pattern where most of the bottom half of the forest is not plated well.

Figure 2.4 Nickel-Plated CNTs with nickel sulfamate bath.



(a) 50 μm scale



(b) 10 μm scale

Figure 2.5 Nickel-electroplated CNTs with a nickel chloride bath.

with the current set to 45%. Ozone is flowed over the CNTs for 30 minutes. Immediately afterwards, oxygen is flowed over the sample for two minutes. Figure 2.6a and 2.6b are micrographs of nickel-electroplated samples that were treated with ozone prior to electroplating.

2.8 Pulsing, Current Density, and Pre-Soak Time

Commonly used in the high-aspect-ratio electroplating industry is pulsing at a constant current source. To try and prevent keyholing, most runs were plated at 3ms on and 27 ms off. The current was run at 8 mA/mm^3. Most electroplating standard operating procedures use square area instead of volume to measure current density. It is difficult to measure the square area of a CNT forest. To be more precise, volume was used instead. Also, to ensure the structure was sufficiently wetted, samples were soaked for 30 minutes before plating began.

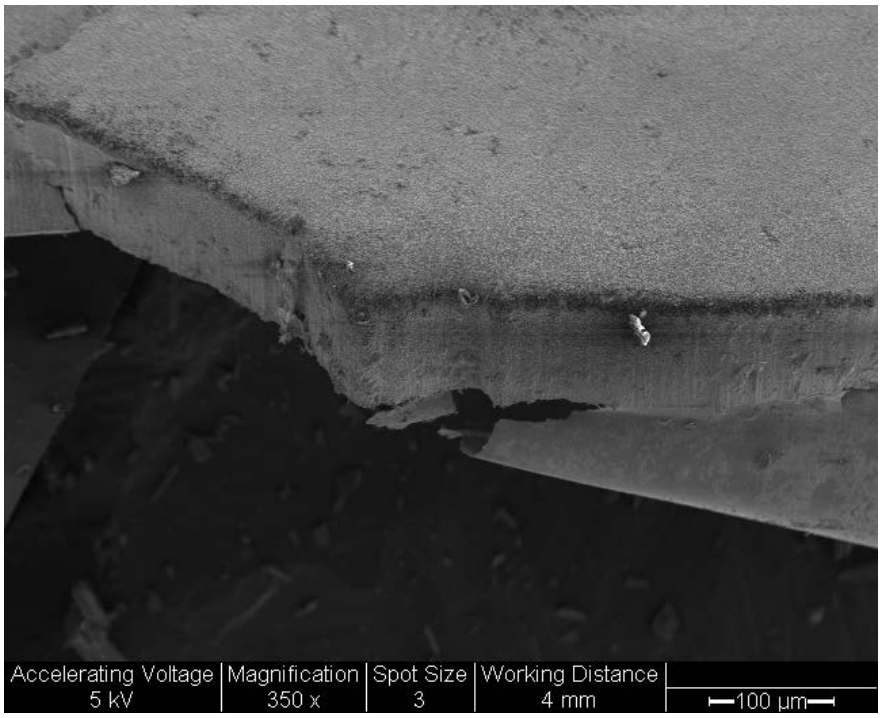
2.9 Final Parameters

There are 12 known variables affecting electroplating. Table 2.2 lists the range of variables that currently provide the most uniform plating.

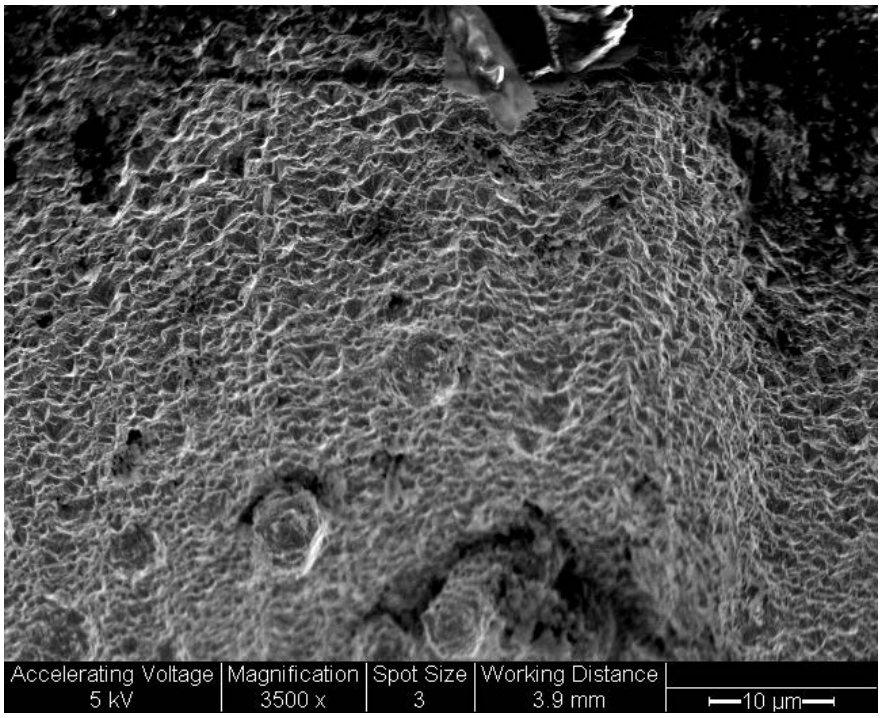
2.10 Material Properties

Fixed-free cantilever beams were fabricated and tested for Young's modulus and ultimate strength. The cantilevers are 500 μm wide and vary in different lengths ranging from 2.5 mm to 4 mm. After these cantilevers were fabricated, they were measured with an Instron table-top tensile tester.

Two different structures have been created to begin measuring material properties. As explained in Lawrence Barrett's senior thesis [1], a structure was created to test the magnetic capabilities material. As a magnet was placed next to the suspended mass, the mass moved toward the



(a) 350x



(b) 3500x

Figure 2.6 Ozone treated CNTs plated with a $NiCl_2$ bath with 350x and 3500x magnifications.

Variable	Parameter Used
Solution	$NiCl_2$ bath
Temperature	50 °C
Starting pH	3-4
Current Density	8 mA/mm^3
Pulsing	3 ms on 27 ms off
Agitation	Magnetic Stir Bar
Electrical Contact	Needle Directly onto CNTs
Anode	Sulphur Depolarized Nickel Rounds
Anode Basket	Titanium mesh
Ozone Surface Treatment	30 minutes
Pre-Soak Time	30 minutes
Run Time	8.5 hours

Table 2.2 Current nickel-electroplating parameters for plating the forest with the most fill.

direction of the magnet, showing that the material was indeed magnetic. A 5 mm x 5 mm x 120 μm sample was nickel-plated, cut, and measured. A sample was measured using an alternating gradient magnetometer.

2.11 Instron Tensile Testing

We have obtained preliminary Instron tensile strength testing results. They are taken by placing a needle on a fixed-free cantilever beam. The Instron machine measures the force versus deflection. Elasticity and strength are then determined by these relations. The results are produced in Table 2.3. It should be noted that this was measured with cantilevers and the stress concentrations at the breaking points were not considered making the values for tensile strength, very conservative.

	Young's Modulus (GPa)	Tensile Strength (MPa)	Density (g/cm^3)
85% Nickel-Plated CNTs	42.4	229-643	7.3-7.98
Other Nickel-Fabrication [14]	200	140-350	8.9
Silicon [14]	168	7000	2.329

Table 2.3 Material properties of nickel and silicon processes used for MEMS.

2.12 Alternating Gradient Magnetometer (AGM)

We have found some basic material properties and a magnetic hysteresis curve. Two samples were prepared at BYU and the magnetic hysteresis curve was measured at UA using an alternating gradient magnetometer (AGM). The results are shown in Figure 2.7. There is a small discrepancy when the sample was measured in the direction parallel to the CNTs.

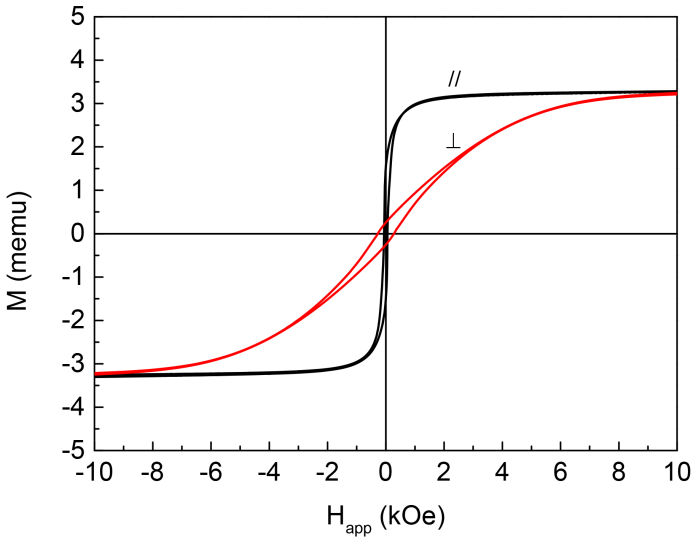


Figure 2.7 A 0.22 mg sample was cut and measured in an alternating gradient magnetometer. Results shown include the magnetic field perpendicular to the sample and parallel to the sample. Note that the magnetic field perpendicular to the sample are parallel to the CNTs.

According to studies done on bulk nickel materials, the nickel-CNT composite appears to magnetically act like a bulk material, not a thin film. Similar AGM graphs can be shown in Edwards [15] for thin films and Korneva et al [16] for bulk material. It qualitatively matches bulk nickel graphs. The shapes of the curves are similar.

For measurements parallel to the substrate, the magnetic field strength is less than expected suggesting that the directionality of the CNTs may be playing a role in the magnetization. For the measurements perpendicular to the sample, the magnetic field strength is greater than expected. Guesses to this cause are paramagnetization of the nickel at high fields, or small amounts of impurities (iron or cobalt) that can change the magnetic properties. [17].



Figure 2.8 Top view of polished annealed nickel-electroplated CNTs. The different shades of grey indicate different grain orientations

2.13 Annealing

As stated previously, the nickel-electroplated CNTs are very brittle and not ductile. As ductility is one of the top reasons for using a metal instead of a ceramic, nickel-electroplated CNTs have been annealed. Samples were place in a 1 in tube furnace, and ramped to 1000°C for 60 minutes, then air cooled. Argon was flowed through the tube during this time.

To compare grain sizes, nickel samples were polished progressivley with a 30 μm grit, a 3 μm grit, 1 μm grit, 0.5 μm grit, diamond spray finished with colloidal silicon and buffing with a fine cloth. Results were then observed using the S-FEG SEM XL-30. Figure 2.8 and Figure 2.9 is a top view and side view respectivley of a sample that is not annealed. Figure 2.10 and 2.11 are top views of a sample that is annealed.

By looking at the contrasts of the different samples, the annealed sample has much larger grains, some of them nearly two to three microns in size. The sample that is not annealed has holes in a range of 50nm in diameter where the CNTs were. There are other holes on the scale of

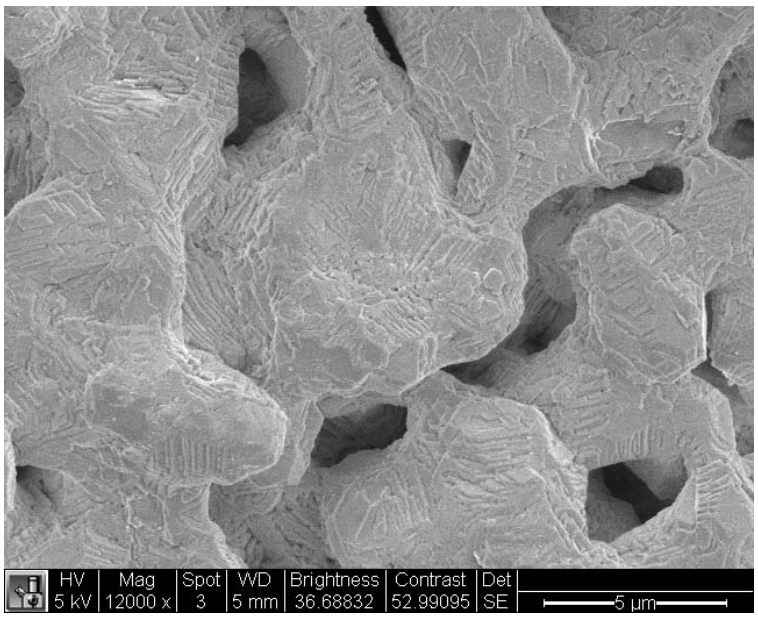


Figure 2.9 Side view of polished annealed nickel-electroplated CNTs. One can notice grooves in the nickel with the same diameter as the CNTs. It is thought that either the CNTs were absorbed into the nickel or reacted with impurities in the argon gas.

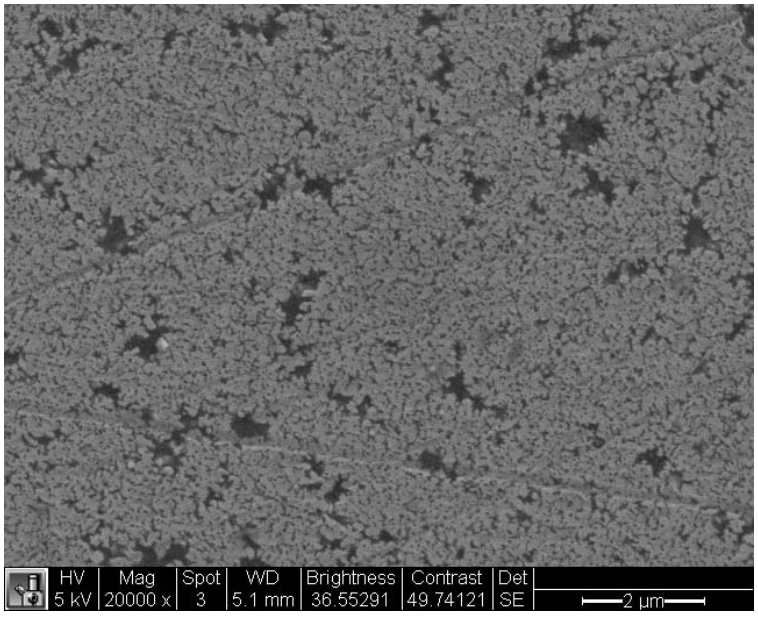


Figure 2.10 Polished nickel-electroplated CNTs at 20000x.

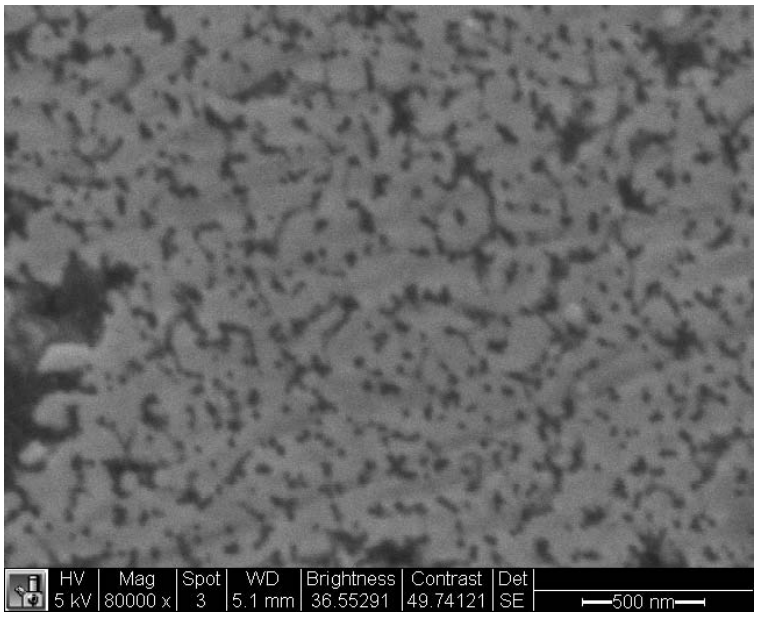


Figure 2.11 Polished nickel-electroplated CNTs at 80000x. The smaller holes are about the size of CNTs. There are also larger gaps demonstrating that while uniform, nickel has not completely infiltrated the forest.

200-300 nm where the nickel appears to be missing. Furthermore, the grain boundaries appear to be less than one μm. These several factors are contributing towards the brittleness of the material.

To help determine grain sizes, the annealed samples as shown in Figure 2.12 has been analyzed using electron backscattered detection (EBSD). As predicted by the SEM graphs, there are large grains in the annealed samples. The sample that is not annealed has not been analyzed yet.

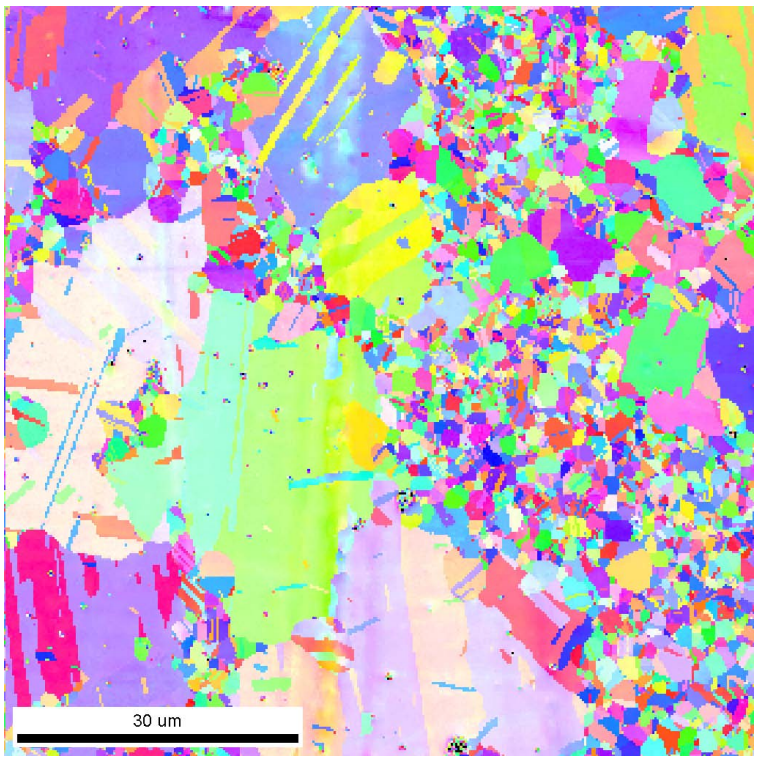


Figure 2.12 A sample of polished annealed nickel-electroplated CNTs with orientation imaging microscopy. The different colors indicate different grains.

Chapter 3

Copper-Electroplating

3.1 Introduction

As electroplating metals onto CNTs are difficult and require a series of different variables, and as electroplating through-silcion vias are difficult, most experiments of copper-electroplating CNTs are not done inside of vias, but rather onto a patterned structure similar to the nickel experiments explained in chapter two.

The same electrical contact for copper-electroplating was used in chapter 2 for nickel-electroplating as shown in Figure 3.1.

All copper-electroplating was performed at the University of Alabama (UA) under the direction of Prof. Susan Burkett and Dr. Ying Feng. As explained in the Chapter 2 covering nickel-plating, the contact device was clipped to the CNT samples. The CNTs were one cm diameter circles with a height at about 120 μm. The samples were submerged in different copper solutions provided by Enthone. Pulse plating was provided by Wafer Power WPT series Single Channel. Temperature and pH was monitored with a multi measuring tool manufactured by Extech. The anode was made of pure copper pickled in a sulphuric acid and common copper etchant rinse before each use.



Figure 3.1 Electrically insulated contact device with a needle on the CNTs.

The current variables used for the most uniform plating are described in Table 3.1.

Variable	Parameter Used
Solution	DVF MU 200, no additives
Temperature	50 °C
Starting pH	0.5
Current	1 mA
Pulsing	5 ms on 50 ms off
Agitation	Magnetic Stir Bar
Electrical Contact	Needle Directly onto CNTs
Anode	Pickled Pure Copper
Anode Basket	None
Ozone Surface Treatment	None
Pre-Soak Time	30 minutes
Run Time	6 hours

Table 3.1 Final copper-plating parameters for plating the forest with the most fill.

Almost all electroplating methods resulted in an effective plating of the outside region. We are interested in plating the whole structure, and not merely coating an outside structure. The samples were mechanically broken with tweezers, and the cross-section was observed using a Lyra TESCAN scanning electron microscope. The following sections will explain how the conclusions in the table were reached.

3.2 Preliminary Copper Solution

The first solution tested was CU Bath SC MD with an additive CU bath LO 70/30. Enthone holds the patent on the chemistry of this design and was unwilling to disclose the contents of their electroplating baths. The solution's Materials Safety Data Sheet (MSDS) showed that the bath had a sulphuric acid base. The solution was designed to copper electroplate TSVs with a high-aspect ratio. This solution was continuously flowed through a filter and kept at room temperature. Current was run at 100 mA 5ms on and 50 ms off. As shown in Figure 3.2, micron sized clumps of copper were deposited in in the middle of the forest. The electroplating is not uniform by any means. It seems that there was a single nucleation site on the CNTs that the copper formed on. Then copper atoms continued to deposit on copper rather than the CNTs. Using this sample of our base, we looked at possible alternatives for solutions and different methods to surface treat the CNTs.

3.3 Ozone Treatment

As explained in chapter 2, ozone assists in electroplating CNTs by changing the natural hydrophobicity of the forests to a hydrophilic state. The procedure is outlined in Jensen et. al. [10]. The system used at BYU is an Atlas ozone generator. Compressed oxygen is flowed through the machine that converts oxygen into ozone. Ozone is then flowed through a tube where the samples are lying. UA did not own one of these machines so we explored the merits of alternate ozone treatments on the CNTs.

One ozone experiment performed was the use of a plasma generator. A small vacuum would be applied to a place where an electric bias would be applied to create a plasma out of the existing air. The proposed ideas is that the plasma would then convert oxygen to ozone. The resulting ozone could then be used to treat the CNTs. The plasma generator was too powerful at it's lowest setting. CNTs were torn from the substrate in some places and completely obliterated in other

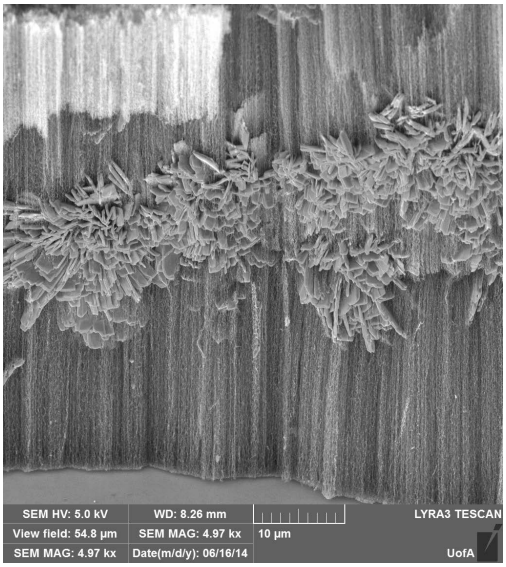


Figure 3.2 CNTs plated with a Cu Bath SC MD and LO 70/30. The plating was performed at room temperature. The sample was cleaved in order to look at the side view cross-section. The stringy part of the structure are the CNTs. The polygonal blocks sticking out of the middle of the forest is copper. The plating of copper here appears random and nonuniform. One thing to note is the strangeness of these blocks. This and other smaples have polygonal blocks sticking out of the CNTs, but we are supposedly looking at the cleaved section in the middle of the forest. One would not see the polygonal blocks clean like that. It would be intuitive to assume one would see broken pieces of CNTs sticking out of the copper. There could have been a crack or gap in the CNTs that allowed the copper to grow unhindered by the CNTs. If this is the case, this would decrease the veracity of the data taken. Further data should be taken using other less destructive, and more precise methods.

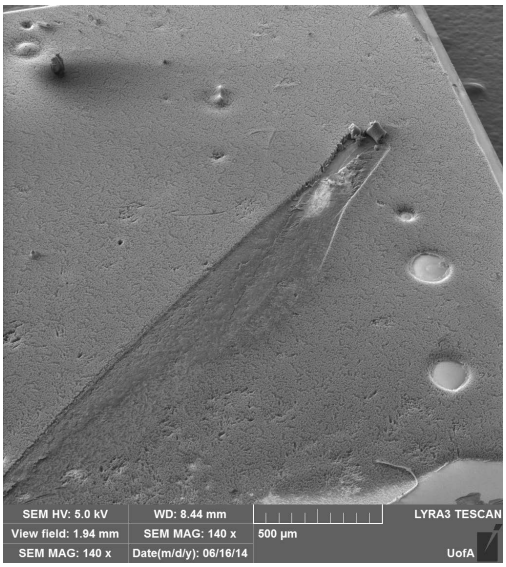


Figure 3.3 CNTs plasma treated for 90 minutes at the lowest possible setting. The plasma caused widespread destruction across the CNTs as can be seen by the torn up strucuture. Judging by the destruction, surface treating CNTs with plasma is irrelevant considering the hundreds of μms of annihilation.

places. Figure 3.3 shows the destruction of plasma treated CNTs.

The other attempt at ozone treatment used a different type of ozone generator called a mercury lamp generator. The theory behind the mercury lamp is that a mercury lamp created high intensity UV light that ozonate the air. No supplementary gases were fed into the system. In Figure 3.4, the reader can notice the pock marks on the the CNTs. The mercury lamp must be causing the CNTs to react with the atmosphere.

With no other possible ways to ozone treat CNTs at UA, experiements of surface treating CNTs were discontinued.

3.4 More Copper Solutions

There are several electroplating baths provided by a specialty chemistry company, Enthone. Concluding that the SC MD and LO 70/30 bath would not provide uniform electroplating, different

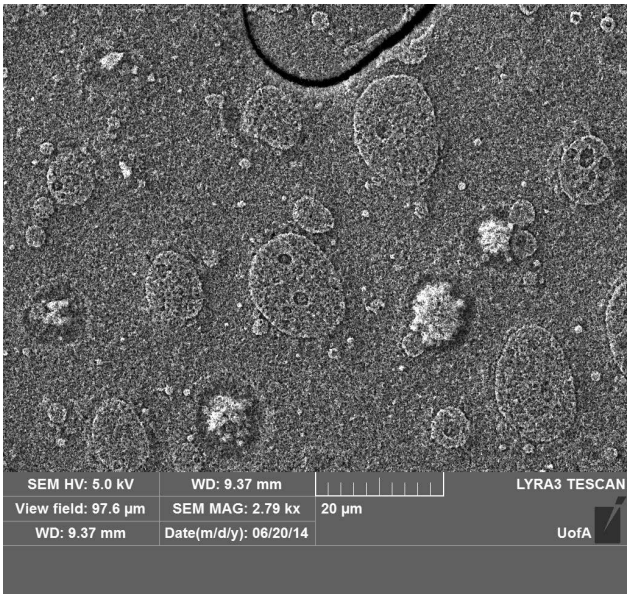


Figure 3.4 CNTs treated with mercury lamp ozone for 90 minutes. The uneven pock marks also make mercury lamp ozone treatment an unlikely candidate for surface treatment.

electroplating baths were used. The base is DVF MU 200 with DVF 200-B and DVF 200-C as additives. As per the recommendations provided by Enthone, 5.5 ml/L of DVF 200-B and 5ml/L of DVF 200-C were added to 200 mL of DVF 200 MU. The solution was kept at room temperature.

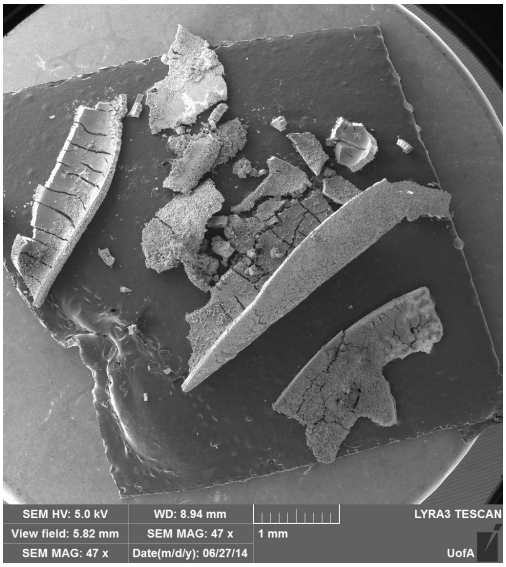
After being rinsed and left out to dry, the one cm circle of CNTs rolled up like a scroll. The structure was weak and brittle. It fell apart as it was mounted in the TESCAN. As shown in Figure 3.5a, there is complete destruction. Copper was deposited on the CNTs, but the internal stress was so great, that it pulled itself in. Figure 3.5b and Figure 3.5c show fissures in the rolled up sample. Zoomed far enough in, one can see copper pellets on the CNTs. This clearly will not work in a TSV application as the structure needs to stay intact inside of the via. With this type of stress, the structures' integrity will be compromised.

Similar to nickel-electroplating CNTs, we found that the accepted standard methods of plating did not work in copper-electroplating CNTs. As such, we attempted to mimic several of the parameters used in nickel-electroplating. As explained in Chapter 2 and shown in Table 2.1, we use

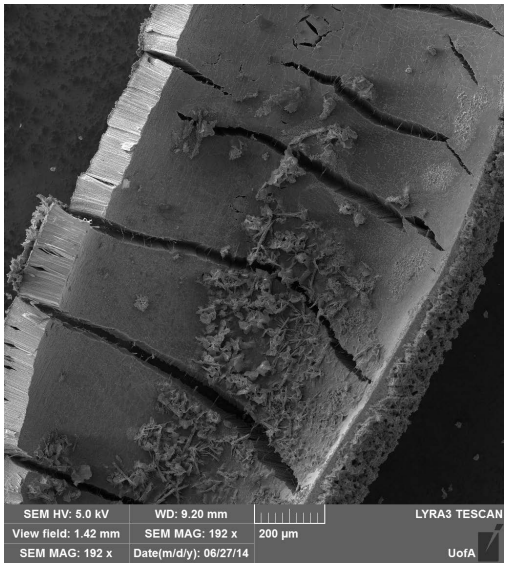
boric acid as a buffer to keep the pH level from changing. As ions are depleted or added, boric acid can donate or accept extra hydrogen atoms to keep the pH stable. A bath of boric acid and dilute solution was created and was subsequently tested. The DVF MU-200 solution with no Enthone additives was diluted 15:1 with deionized water and 10g/L boric acid was added. The solution was heated to 50°C. There are much smaller grains as shown in Figure 3.6, but the forest was not filled all of the way.

An even more dilute solution was created to significantly raise the pH. A 121:1 water to DVF 200 MU solution with no additives was created resulting in a pH of 2.7. Figure 3.7b shows the result. The pH was 3.7. However, this method greatly reduces the concentration of copper ions in solution. There are several small beads, but a plating run of several days would need to be conducted to determine the usefulness of this solution. The plating machine was incapable of running for several days, so this process was abandoned.

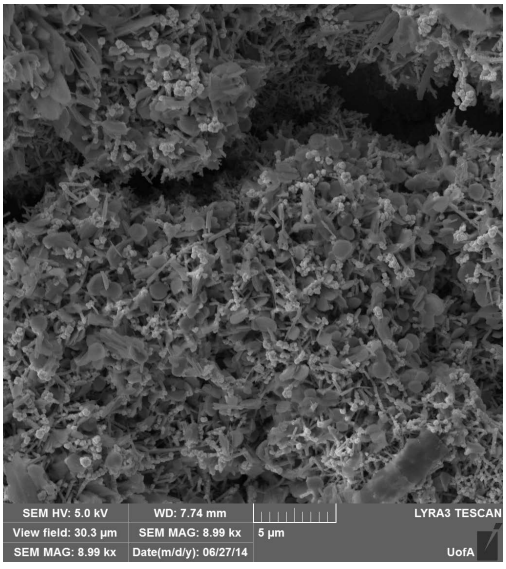
Eventually, no additives were added and only the DVF MU 200 solution was used. The solution was heated to 50°C, the current was 1 mA, and it was plated for six to eight hours. Figures 3.8a and 3.8b show the results.



(a) 88x Mag



(b) 192x Mag



(c) 8.99 kX Mag

Figure 3.5 CNTs plated with a copper-bath with a base of MU 200-B and MU 200-C from Enthone.

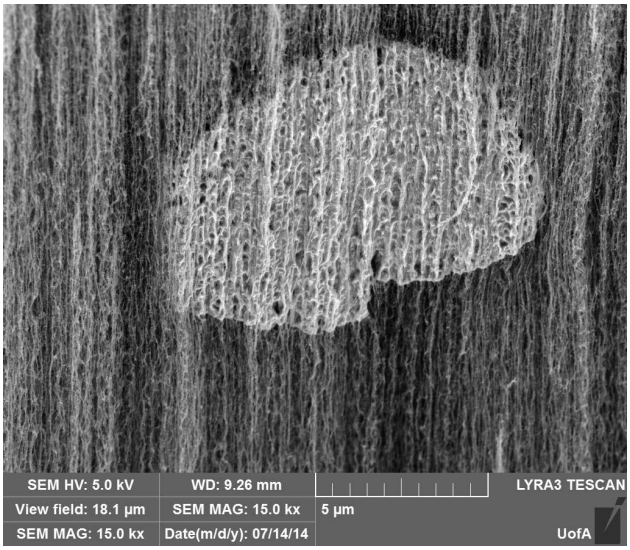
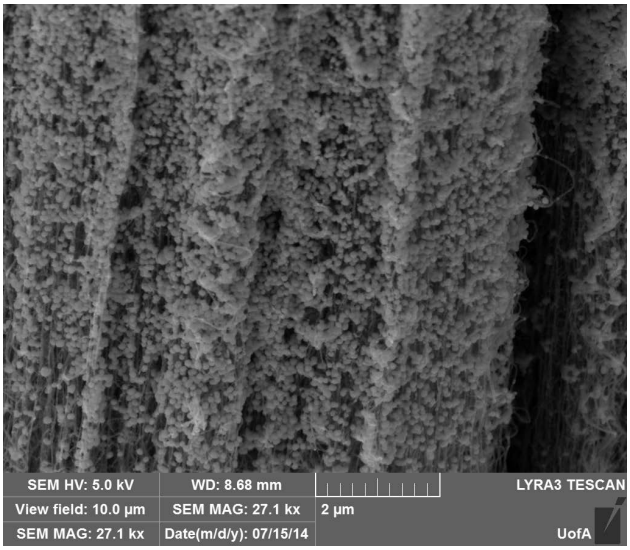
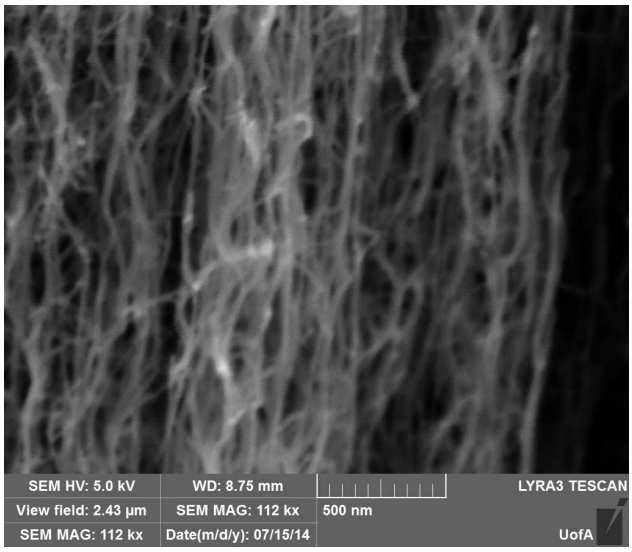


Figure 3.6 Copper-plated CNTs with DVF MU 200 diluted 15:1 with deionized water and with 10g/l of boric acid added. The solution was kept at 45 °C.

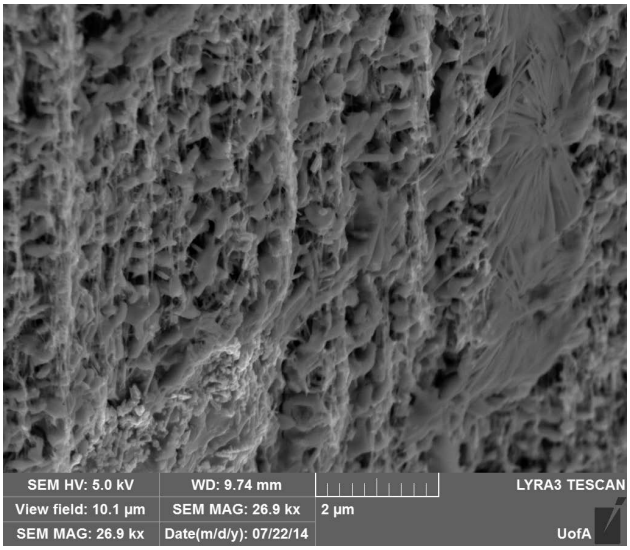


(a) 1mA current was pulsed 5ms on and 50ms off. The sample was plated for about 6 hours. This is near the top of the forest

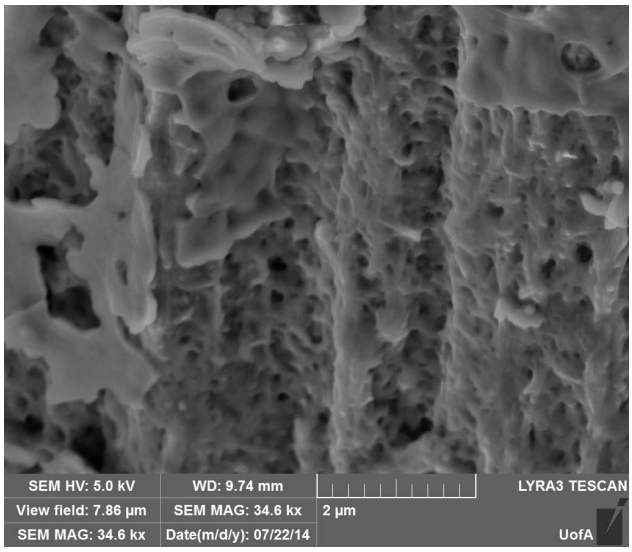


(b) This is near the bottom of the forest.

Figure 3.7 Copper-plated CNTs with DVF MU 200 diluted 121:1 with de-ionized water.



(a) DVF MU 200 with no additives. The bath was plated at 50 °C, for 1mA 3ms on and 30ms off. This had four minutes of carbon infiltration.



(b) A different part of the forest.

Figure 3.8 Copper-plated CNTs with DVF MU 200 with no additives

Chapter 4

Future Work

As many of the conclusions were drawn in the results, this chapter will take the conclusions made and will introduce ideas for some further work.

4.1 Ideas for Continuing Nickel

We have found some basic material properties and a magnetic hysteresis curve. Two samples were prepared at BYU and the magnetic hysteresis curve was measured at UA using an alternating gradient magnetometer (AGM). As it was one sample, it is not included in this thesis, but the next step is to prepare more samples and have them tested with an AGM to gave magnetic properties tested.

Efforts should be put in for repeatablility. In nearly all of the experiments, there was about a 50% fail rate where there was a short, wires were crossed, or some other unexplained reason for failing to plate as expected, most often in little to no plating at all. There was a lot of evaporation in both the nickel and copper baths as the tops of the containers were open. While evaporation was reduced by covering the top with plastic, this could be an unintended variable. The next electroplating baths should include a more fully closed container.

Another clipping method should be explored. Macroscopically, nail polish was not observed to disolve in the electroplating baths, but that is not for certain. Securing the sample may be done easier if the sample was attached to a substrate with an adhesive then the electrical connection be brought separately.

There is a need for stastically significant quantitative data. Most of the thesis is very qualitative in nature with few graphs to back up conclusions. More tests should be done to give weight to the current results.

At 85% density, nickel-electroplated CNTs do not deform plastically like bulk nickel does, but the Young's modulus of our fabrication process is an order of magnitude lower than the Young's modulus of bulk nickel making it more flexible. Along with magnetization, ductility, the ability for a material to continue to bend after it is permamently deformed, is a factor for choosing a metal as a material for devices. The nickel-electroplated CNTs are currently brittle. Annealing samples could make them more ductile opening the doors to further application.

4.2 Ideas for Continuing Copper

The copper-electroplating solution has a sulfuric acid base. The sulfuric acid did not react with the nail polish alone especially in thick quantities, but the staple would fall off of the clip after each run. It was interpreted as being merely a cold solder joint until it was later learned that copper sulfamate solution is often the solution of choice to etch zinc and tin. After soaking several sharp objects (pushpins, paperclips, and staples) and solder in the DVF 200 MU bath, it was found that all of the objects were corroded after a period of a few hours. The pushpin survived the best as it was the thickest. Solder was all but dissolved away. A different connecting method with a metal non-reactive to sulphuric acid to make electrical connection ought to be used for long-term copper plating with this solution.

While possible at BYU, it is difficult to ozone treat samples without an ozone generator. Furthermore, if these experiments are to be repeated at another university, an Atlas ozone generator is expensive to purchase. Reports have outlined treatments other than ozone that could surface treat the CNTs. Nitric acid is used to make the CNTs hydrophilic and oxidizes the CNTs well. Using nitric acid could replace ozone in surface treatments The CNTs are also etched so the process would have to be all at once: Nitric Acid etch followed by a rinse, and plating before it was allowed to dry might work. Pickling is a process to clean surfaces before electroplating, often with acids. Pre-treating samples with an acid such as nitric acidwould likely be an acceptable substitute for ozone treatment in a manufacturing process.

If the copper in the copper anode is pure, the same amount of copper ions at the anode are released into the solution at the same rate as they are plated at the cathode. This creates a problem as it is difficult to keep the current densities of the anode and cathode the same. At BYU, this problem seemed to be fixed with the introduction of sulphur depolarized nickel rounds. Hopefully, the phosphorized copper anode will be able to accomplish the same thing. This should be prioritized for the next step in trying to copper-electroplate CNTs.

All of Enthone's copper-electroplating baths have a sulphuric acid base. The history of copper-plating baths, however, has not been limited to sulphuric acid solutions only. There have been other instances of copper-plating solutions including copper flouborate and copper cyanide. While these might end up being more hazardous than sulphuric acid based baths, it would be interesting to test the different solutions. DVF 200 MU copper-electroplating bath has a pH at around 0.5. This is more acidic than most acids, let alone electroplating baths. The nickel-electroplating bath used has a pH of 3-4. Pourbaix created diagrams showing pH, voltage, and stability. That is, as a pH/voltage combination reaches an extreme, corrosion, ionization, or gas bubbling will be more likely [18]. As the pH for DVF 200 MU is extremely low, this may be affecting the CNTs adversely.

One can densify CNTs using acetone or IPA. Done correctly, this could just require the outside

to be plated with no attempts at filling the inside of the forest and still provide the structure necessary. One run was done and electroplated. The sample was destroyed, so we diverted our attention to different ideas, but densification should be explored again.

4.3 Wrap-up

Using a complex series of parameters, metal electroplating CNTs will be able to provide a new process for fabricating high-aspect ratio metal structures. Once optimized for production, these new metal-composite devices will be expanded into industrial and commercial markets improving actuators, sensors, and integrated circuits.

Appendix A

Patterned Carbon Nanotube Forest Growth

1. Begin with a polished silicon wafer with a (100) lattice structure.
2. Deposit 30nm of alumina on the silicon wafer by electron beam evaporation under 50 μtorr.
3. Spin AZ-3030 postive photoresist.
4. Pattern the photoresist with a Karl Suss Mask Aligner MA 150 CC.
5. Deposit 7nm of iron by thermal evaporation under 100 μtorr.
6. Place sample in a 1-in quartz tube furnace (Lindberg Blue M EW-33850) tube furnace.
7. Heat from room temperature to 750°C while flowing 220 sccm of hydrogen to remove oxygen atoms (a process called reducing). The iron at this point is also turning from a thin film into individual nanoparticles allowing the metal to act as a catalyst [19]. Reaching 750°C takes approximately 10 minutes.
8. When the furnace reaches 750°C, keep the hydrogen flow constant and flow 260 sccm of ethylene, C_2H_4, for 2 minutes resulting in patterned CNTs.
9. Ramp the furnace temperature to 900°C. Reaching 900°C takes about four minutes.

10. Flow ethylene at the same rate as before to deposit nano-crystalline carbon on the forest.

11. Cool while flowing hydrogen. The furnace is slowly cooled in 12 minutes to 700 °C, then it is opened and cooled quickly with a fan.

Bibliography

[1] L. K. Barrett, "High-Aspect-Ratio Metal Microfabration by Nickel Electroplating of Patterned Carbon Nanotube Forests," Senior Thesis (Brigham Young University, Provo, 2014).

[2] L. K. Barrett, D. J. Barton, S. G. Noyce, D. D. Allred, R. R. Vanfleet, and R. C. Davis, "High-Aspect-Ratio Metal Microfabrication by Nickel Electroplating of Patterned Carbon Nanotube Forests," Journal of Microelectricalmechanical Systems (2015).

[3] D. Niarchos, "Magnetic MEMS: key issues and some applications," Sensors and Actuator A: Physical (2003).

[4] I. Present, "Cramming more components onto integrated circuits," Readings in computer architecture p. 56 (2000).

[5] J. Taylor, C. Zafiratos, and M. Dubson, in *Modern Physics for Scientists and Engineers*, 2nd ed., J. Challice, ed., (Pearson Education, Upper Saddle River, 2004), pp. 466–473.

[6] M. Rahimian, A. A. Orouji, and A. Aminbeidokhti, "32 nm high current performance double gate MOSFET for low power CMOS circuits," International Journal of Electronics **102,** 347–361 (2015).

[7] H. Shahnazarisani and S. Mohammadi, "Simulation analysis of a novel fully depleted SOI MOSFET: Electrical and thermal performance improvement through trapezoidally doped

channel and silicon-nitride buried insulator," Physica E: Low-dimensional Systems and Nanostructures (2015).

[8] S. Burkett and L. Schaper, in *3D Integration: Technology and Applications*, P. R. P. Garrou and C. Bower, eds., (Wiley, 2008).

[9] B. H. Hanna, W. C. Fazio, J. D. Tanne, J. M. Lund, T. S. Wood, R. C. Davis, R. R. Vanfleet, and B. D. Jensen, "Mechanical Property Measurement of Carbon Infiltrated Carbon Nanotube Structures for Compliant Micromechanisms," Journal of Microelectrical Mechanical Systems **23,** 1330–1339 (2014).

[10] D. S. Jensen, S. S. Kanyal, N. Madaan, A. J. Miles, R. Davis, R. R. Vanfleet, M. A. Vail, A. E. Dadson, and M. R. Linford, "Ozone priming of patterned carbon nanotube forests for subsequent atomic layer deposition-like deposition of SiO2 for the preparation of microfabricated thin layer chromatography plates," Journal of Vacuum Science & Technology B **31,** 031803 (2013).

[11] H. Wang, Z. Huang, Q. Cai, K. Kulkarni, C. L. Chen, D. Carnahan, and Z. Ren, "Reversible transformation of hydrophobicity and hydrophilicity of aligned carbon nanotube arrays and buckypapers by dry processes," Carbon **48,** 868–875 (2010).

[12] Y. Tsuru, M. Nomura, and F. Foulkes, "Effects of boric acid on hydrogen evolution and internal stress in films deposited from a nickel sulfamate bath," Journal of Applied electrochemistry (2002).

[13] J. Ji, W. Cooper, D. Dreisinger, and E. Peters, "Surface pH measurements during nickel electrodeposition," Journal of Applied Electrochemistry (1995).

[14] C. Liu, *Foundations of MEMS*, 2nd ed. (A Gilfillan and A. Dworkin, Upper Saddle River, 2012).

[15] R. L. Edwards, "The Magnetic Properties of Evaporated Nickel and Iron Films," Physical Review **29,** 321–333 (1927).

[16] G. Korneva, H. Ye, Y. Gogotsi, D. Halverson, G. Friedman, J. C. Bradley, and K. G. Kornev, "Carbon Nanotubes Loaded with Magnetic Properties," Nanoletters **5,** 879–884 (2005).

[17] T. Suzuki, Private communication (2015).

[18] M. Pourbaix, *Atlas of electrochemical equilibria in aqueous solutions* (New York Pergamon Press, Oxford, 1966).

[19] S. Naha and I. K. Puri, "A model for catalytic growth of carbon nanotubes," Journal of Physics D: Applied Physics 41 (2008).

Index

AGM, 17
anode, 14, 23, 25, 37

boric acid, 10

cooper flouborate, 37
copper cyanide, 37

die, 3

electromigration, 3
Enthone, 28, 29, 37

granite, 2

hydrophobic, 11, 26

instron, 17
internal stress, 10

magnetic hysteresis, 17
MEMS, 1, 2, 17
MOSFET, 3

nickel chloride, 10, 11, 14
nickel sulfamate, 10, 11
nitric acid, 36
non-uniform, 10

ozone, 11, 14, 26, 28

pH, 14, 25, 37
phosphorized, 37
photoresist, 39
Pourbaix, 37
pure, 23, 37

quantum tunneling, 3

saccharin, 10
sodium sulfate, 10

tensile strength, 17
throwing power, 10
transistor, 3

uniform, 11, 23, 26

Young's Modulus, 17